Journal of Molecular Catalysis A: Chemical 287 (2008) 9–15

Contents lists available at ScienceDirect

Journal of Molecular Catalysis A: Chemical

journal homepage: www.elsevier.com/locate/molcata

Synthesis of dipropyl carbonate by transesterification over KNO_3/MCM-48

Yongxin Li[a,*], Yanhua Zhang[b], Bing Xue[a], Yuhua Guo[a]

[a] Department of Chemical Engineering, Jiangsu Polytechnic University, Changzhou, Jiangsu 213164, PR China
[b] School of Material Science and Engineering, Tianjin University, Tianjin 300072, PR China

ARTICLE INFO

Article history:
Received 11 December 2006
Received in revised form 21 January 2008
Accepted 13 February 2008
Available online 19 February 2008

Keywords:
Potassium nitrate
MCM-48
Transesterification
DMC
Dipropyl carbonate

ABSTRACT

The catalytic behavior of the mesoporous sieve supported potassium nitrate KNO_3/MCM-48 for the synthesis of dipropyl carbonates (DPC) by transesterification of dimethyl carbonate (DMC) with propanol was investigated. The catalysts were characterized by the techniques of X-ray diffraction (XRD), CO_2 temperature-programmed desorption (CO_2-TPD), FT-IR spectroscopy, N_2 adsorption and X-ray fluorescence (XRF). The XRD results indicated that the structure of MCM-48 was gradually deformed with the increase in the KNO_3 loading, whereas the framework of MCM-48 was basically retained until the loading of KNO_3 was over 18%. IR spectra showed that KNO_3 was gradually decomposed with increasing calcination temperature. The CO_2-TPD showed two new types of basic site were generated, which have higher catalytic ability for the synthesis of DPC. Effects of the loading amount of active components, the calcinatory temperature, the catalyst dosage and the reaction conditions on the catalytic activity were investigated in detail and the optimized reaction conditions were acquired.

1. Introduction

Dipropyl carbonate (DPC), which contains both propoxy and carbonyl groups, could be served as an important precursor for polycarbonate as well as a useful propylating and propoxycarbonylating agent for the syntheses of numerous organic products. Owning to their high dielectric constants, dialky cabonates are wildly used as electrolytes in lithium batteries. Due to its larger molecular weight, higher flash point and stronger antioxidation than that of dimethyl carbonate (DMC) and diethyl carbonate (DEC), DPC is a more stable and safe electrolyte for lithium batteries.

To our knowledge there has not been any report about the synthesis of DPC yet. Although there are some reports on the preparations of other dialkyl carbonates [1–3], these synthetic approaches have many disadvantages. Dialkyl carbonates are usually prepared using toxic phosgene and the by-products include hydrochloric acid and other chlorides, which present serious corrosion and disposal problems, and the conversions of starting materials are always very low.

Dimethyl carbonate, which is hardly toxic and nicely biodegradable, is an important raw material in organic synthesis and has drawn more and more attention from researchers [4–14]. Owing to the presence of two methoxyl groups and a carbonyl group in a molecule, DMC has been used as an effective carbonylation agent to replace the virulent phosgene for manufacturing plastic polycarbonates and also used as an useful methylating agent to replace hazardous dimethyl sulfate. Particularly, the application of DMC as carbonylating agent is very attractive due to its ability to overcome the drawbacks of carbonylation with phosgene as the carbonylating agent [15–19], such as a long industrial process, complex techniques, high toxicity, serious pollution and excessive by-products. In our research, the synthesis of DPC by transesterification from DMC with propanol is an environmental benign process, in which the nontoxic chemical reagent DMC was used as the carbonylation agent.

The preparation and application of mesoporous molecular sieve MCM-48 have attracted much attention from both practical and theoretical points [20–35]. However, there are only a few reports on its use as a catalytic component, especially for a solid base catalytic system. It is also a prospective catalytic component in liquid-phase reaction due to its three-dimensional mesoporous channeling structure [36], which is more resistant to pores blockage and therefore allows faster diffusion. In our research, the synthesis of DPC catalyzed by MCM-48 supported potassium nitrate showed very high conversion of DMC and selectivity for DPC.

There is no precedent for MCM-48 supported solid base catalyst being used in synthesis of DPC by transesterification from DMC with propanol. The effects of the loading amount of active components, catalyst dosage, calcination temperature and reaction time on the

* Corresponding author. Tel.: +86 519 86330135; fax: +86 519 86330135.
E-mail address: liyx@em.jpu.edu.cn (Y. Li).

1381-1169/$ – see front matter © 2008 Elsevier B.V. All rights reserved.
doi:10.1016/j.molcata.2008.02.009

reaction profile were studied in detail and suitable reaction conditions for DPC synthesis were worked out. Furthermore, a plausible mechanism for the transesterification of dimethyl carbonate with propanol over solid basic catalysts was proposed.

2. Experimental

2.1. Materials

Cetyltrimethylammonium bromide (CTAB, Aldrich), tetraethyl orthosilicate (TEOS, Aldrich), NaOH (Aldrich), $Al_2(SO_4)_3{\cdot}18H_2O$(Aldrich), KNO_3 (Aldrich), and deionized water (self-prepared, $R > 8\,M\Omega$).

2.2. Catalyst preparation

The MCM-48 support was prepared by the hydrothermal method [20]. Sodium hydroxide and CTAB were dissolved in deionized water in certain ratio and the mixture was stirred at about 308 K for about 40 min, then tetraethyl orthosilicate was slowly added. The molar composition of the sol was 1TEOS/0.48NaOH/0.415CTAB/55H_2O. The reaction mixture was stirred for about 1 h and then autoclaved for 3 h in a Teflon-lined stainless steel vessel and the temperature was maintained at 383 K for a period of time. The resulting white solid mass was filtered and washed with deionized water in small portions. After drying in air at ambient temperature the sample was calcined at 823 K for 6 h.

The different loadings of KNO_3/MCM-48 were produced by impregnating the mesoporous MCM-48 with aqueous solution of KNO_3. The supported MCM-48 was subsequently dried at 383 K and calcined at a certain temperature. The samples prepared were denoted as KNO_3/MCM-48. The total conent of the metal potassium was 1–25% by weight based on the weight of MCM-48.

2.3. Characterization techniques

Powder X-ray diffraction (XRD) patterns were recorded using a Rigaku D/MAX-PC220 powder diffractometer with Cu Kα radiation (40 kV, 30 mA), 0.5°per min. The nitrogen adsorption–desorption isotherms of support were determined at 77 K on a Micromeritics ASAP 2010 apparatus. The BET specific surface area was calculated using the BET equation for relative pressures in the range $p/p_0 = 0.02$–0.2. The pore size distribution of the sample was determined using the BJH method. FT-IR spectra were measured on a Bruker TENSOR 27 spectrometer in KBr pellets over the range of 400–4000 cm^{-1} with resolution of 1 cm^{-1}. The X-ray fluorescence (XRF) patterns were studied by a XGT-2700 microscope. The basicity of the samples was measured by CO_2 temperature-programmed desorption (CO_2-TPD). A 0.100 g sample was pre-treated at 773 K for 1 h in dry He flow (30 ml/min), and cooled to room temperature, then exposed to pure CO_2 (99.99%) for 0.5 h. After purging the catalyst with He for 0.5 h, the TPD profile was obtained at a heating rate of 10 K/min from room temperature to 773 K. The TCD signal and temperature corresponding to CO_2 desorbed were recorded simultaneously. The amount and temperature of the desorbed CO_2 correspond with the amount and strength of the basic sites qualitatively.

2.4. Transesterification of DMC with propanol

Transesterification of DMC with propanol was carried out in a one-neck flask (250 ml) equipped with a string distillation apparatus and a thermometer. The supported catalyst was charged in this flask along with a liquid mixture of propanol/DMC with an initial mole ratio of 4/1. The reaction was conducted at 363 K at an atmospheric pressure. We assume that the dipropyl carbonate may be synthesized via the following stepwise transesterification:

$$CH_3OCOCH_3 + C_3H_7OH \underset{}{\overset{KNO_3/MCM\text{-}48}{\rightleftharpoons}} CH_3OCOC_3H_7 + CH_3OH \quad (1)$$

$$CH_3OCOC_3H_7 + C_3H_7OH \underset{}{\overset{KNO_3/MCM\text{-}48}{\rightleftharpoons}} C_3H_7OCOC_3H_7 + CH_3OH \quad (2)$$

Owing to the application of the distillation apparatus the continuous separation of co-product methanol from the reaction became feasible; the thermodynamic equilibrium in Eq. (1) was disrupted in favor of DPC formation. Throughout the reaction nitrogen gas was used to purge the reaction vessels first and then protect the system from air. Quantitative analysis of reaction products was carried out on a SP-2100 gas chromatograph (GC) from Beijing Analysis Apparatus Corporation equipped with a flame ionization detector (FID). A polyglycol-packed column was used to separate products for GC analysis.

3. Results and discussion

3.1. Structural analysis of MCM-48 support

FT-IR spectra of MCM-48 support samples are shown in Fig. 1, which demonstrate typical features of its kind [37,38]. The major bands at 1200, 1040, 770 and 440 cm^{-1} were assigned to symmetric and asymmetric Si—O—Si stretching vibrations. The band at 960 cm^{-1} was generally assigned to a Si—O stretching vibration of Si—O—R^+ groups in the as-synthesized state and to Si—OH in the calcined state [39] as well. The broad band in the range of 3200–3800 cm^{-1} was assigned to the internal hydroxyl groups near the surface, and the band around 1650 cm^{-1} was attributed to the bending of water molecules. The bands at 2925, 2850 and 910 cm^{-1} in the as-synthesis sample were due to the stretching vibrations of CH_2, CH_3 and C—N bonds in the surfactant. The bands at 1390 and 1487 cm^{-1} were assigned to the bending vibration of CH_2 of the surfactant. All these signature vibrations were characteristic of the mesoporous MCM-48 structure. After calcination, the three bands disappeared due to the removal of the surfactant.

XRD patterns of the as-synthesized and calcined MCM-48 (Fig. 2) exhibited well-definited reflections [37,38], which were characteristic of the cubic MCM-48 structure [40]. After calcination the intensity of the (2 1 1) peak was obviously enhanced and all XRD peaks were shifted to higher degrees, which indicated that the pores of MCM-48 support shrank during the calcinations.

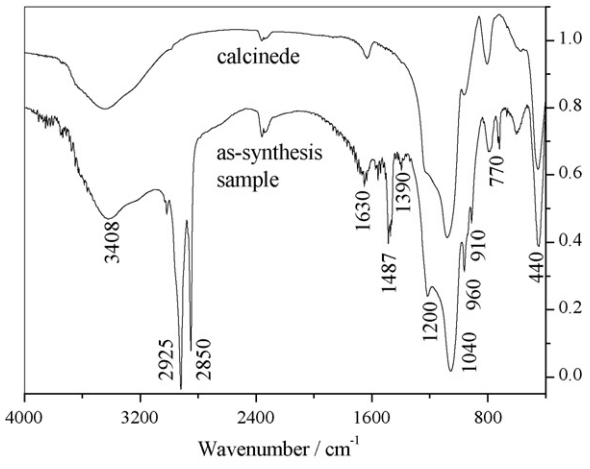

Fig. 1. IR spectra of support MCM-48.

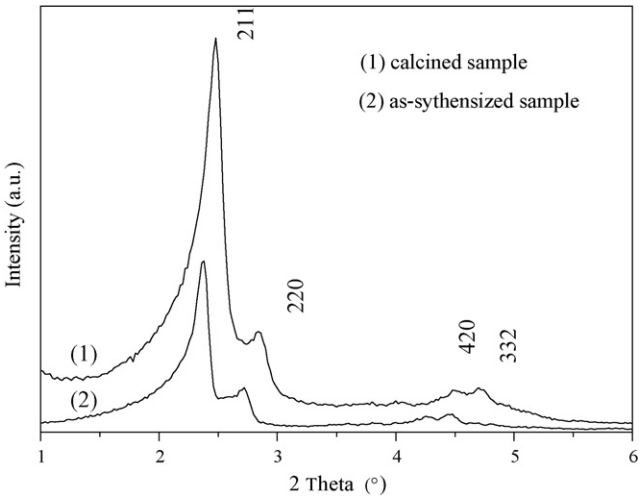

Fig. 2. XRD patterns of support MCM-48.

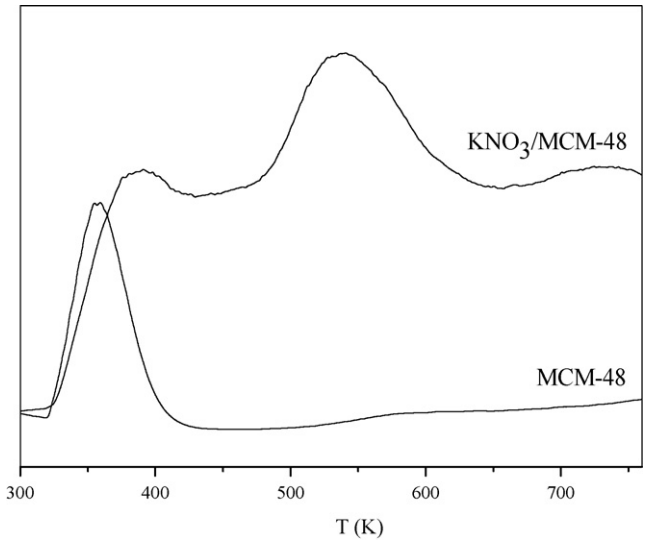

Fig. 4. CO_2-TPD patterns of the catalysts.

The calcined MCM-48 support displayed well-developed type IV nitrogen sorption isotherms. The sample contained a large surface area of 1441.6 m^2/g and a pore size about 3.24 nm.

3.2. Catalytic performance of KNO_3/MCM-48 in the synthesis of DPC

3.2.1. Effect of potassium loadings

The relationship between the potassium loading and the catalytic activity is shown in Fig. 3. It shows that the conversion of DMC was extraordinary high even though the potassium loading was merely 5% and that the catalytic performance was not drastically improved with the increase in the potassium loading from 5% to 18%. It was indicated that the effect of the potassium loading on the conversion of DMC was not significant due to the exceedingly high activity of the catalyst. The selectivity of DPC was optimal at 15% potassium loading, beyond that the yield of DPC decreased with the increase in the potassium loading. Considering both the DMC conversion and the DPC selectivity, the catalyst with a 15% potassium loading showed the best catalytic activity for this reaction.

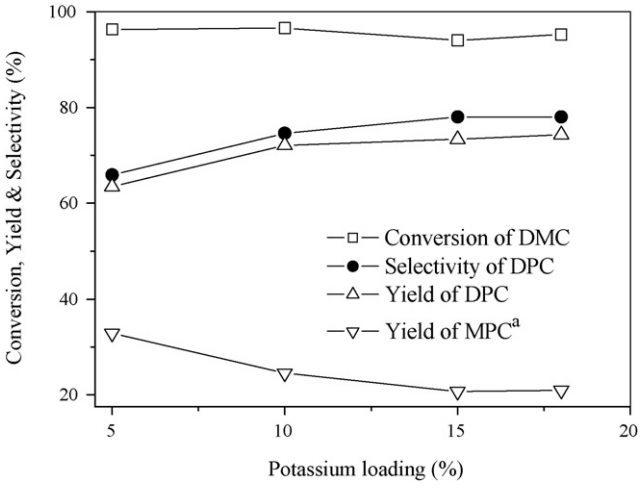

Fig. 3. Effect of potassium loading on conversion of DMC and yield of DPC over KNO_3/MCM-48 at 363 K, catalyst dosage 5%, reaction time 6 h, feed ratio 4:1 (propanol:DMC) and calcination temperature 773 K.
[a] methyl propyl carbonate.

In order to investigate the effect of the basic property of the catalysts on the transesterification of DMC with propanol, CO_2-TPD characterization was conducted. Fig. 4 represents the strength of basic sites on the pure MCM-48 and 15% KNO_3/MCM-48. Only one desorption peak at 350 K emerged in the CO_2-TPD profiles of MCM-48, suggesting the existence of only one type of adsorption sites for CO_2 on this material. MCM-48 possesses large surface areas and plenty of pores, which caused the weak adsorption of CO_2 [41]. The amount and temperature of CO_2 desorbed from the catalyst during CO_2-TPD was dramatically increased by loading 15% KNO_3, which was similar to the result of KNO_3/Al_2O_3 [42]. Since it was reported that the peaks in the high temperature region above about 673 K can be attributed to the desorption of CO_2 from the strong basic sites, the peaks in the temperature between 450 and 673 K can be attributed to the desorption of CO_2 from the intermediate basic sites, and the peaks in the temperature below 450 K can be attributed to the desorption of CO_2 from the weak basic sites [43]. When the MCM-48 was loaded with 15% KNO_3, two new CO_2 desorption peak appeared at the temperature over 550 and 700 K. These results indicated that the remarkable improvement have occurred in both the amount and strength of basic sites on the KNO_3/MCM-48 [44]. Therefore, there must exist strong and intermediate basic sites on KNO_3/MCM-48, while the amount of intermediate basic site was larger than the strong basic site. This basicity, especially for the intermediate basic sites, was the cause of the high activity of the catalyst.

We tested the catalytic activity of an MCM-48 sample without KNO_3 loading in the transesterification of DMC with propanol under the same reaction conditions. In the absence of KNO_3, the MCM-48 sample did not present any catalytic activity, as expected, due to the lack of basic sites on which the transesterification reaction could occur. However, after the 15% KNO_3 was loaded on the MCM-48 the catalysts were active and exhibited a higher catalytic activity as shown in Fig. 3. As illustrated in Fig. 4, the basicity change profiles indicated that the loading of KNO_3 was crucial for the generation of basic sites on the catalyst. KNO_3 can be decomposed when the temperature was over 773 K and K_2O was the decomposition product [45]. It was very likely that the K_2O derived from KNO_3 and dispersed on MCM-48 was the main basic sites, which is important for the transesterification of DMC with propanol.

The effect of the potassium loading on the structure of MCM-48 support is shown in Fig. 5. The results showed that the

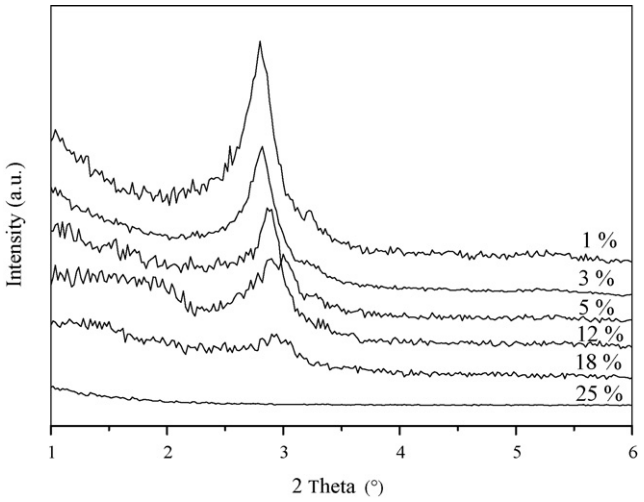

Fig. 5. XRD patterns of MCM-48 with different KNO_3 loadings calcined at 773 K.

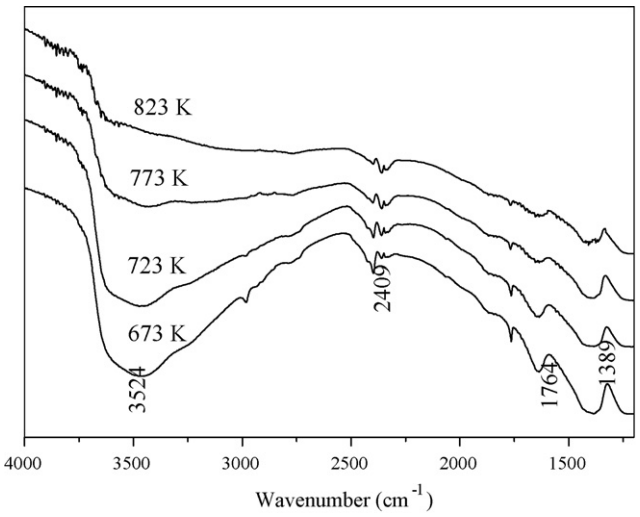

Fig. 7. IR spectra of KNO_3/MCM-48 calcined at different temperatures.

characteristic peaks of MCM-48 were gradually reduced with the increase in the KNO_3 loading from 1% to 25% on MCM-48, which indicated that the structure of MCM-48 support was gradually destroyed when the loading of potassium increased. The basal (2 1 1) and (2 2 0) peaks still existed even though the loading of potassium was as high as 18%, which indicated that the structure of MCM-48 was still survived. Neither KNO_3 nor new phases such as K_2O were observed in the XRD patterns of MCM-48 samples loaded with potassium ranging in amount from 1% to 25%. When the salt or oxide loading is lower than the threshold, it will be in a monolayer state and XRD undetectable [46]. In the XRD patterns of the 35% KNO_3/Al_2O_3 sample calcined at 773 K the K_2O phase was detected obviously [45]. Based on these XRD results, we think that the MCM-48 has a good spontaneous dispersion capacity of KNO_3. The XRD undetectable phase of KNO_3 and K_2O may have dispersed onto the surface of MCM-48 as a monolayer, probably due to the large surface area of MCM-48. Thus, it is clear that the increase in K_2O species can be consistent with an increase in the number of basic sites (Fig. 4), resulting in the increase in the catalytic activity. The identical XRD patterns of the corresponding zeolite indicated a good dispersion of KNO_3 on zeolite, like on KNO_3/NaY [42].

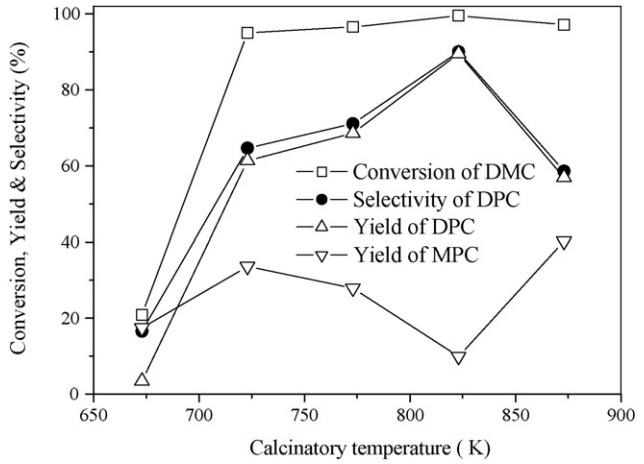

Fig. 6. Effect of calcination temperatures on conversion of DMC and yield of DPC over 15% KNO_3/MCM-48 at 363 K, catalyst dosage 5%, reaction time 6 h and feed ratio 4:1 (propanol:DMC).

3.2.2. *Effect of calcination temperature*

Fig. 6 shows the effect of calcination temperature on the catalytic activity of KNO_3/MCM-48. When calcination temperature changed from 673 to 873 K, the activity of the catalyst exhibited a maximum at calcination temperature of 823 K. The conversion of DMC increased with the increase in calcination temperature and then kept steady beyond 723 K. However, the yield of DPC showed a maximum at 823 K. IR spectra of KNO_3/MCM-48 calcined at different temperatures are presented in Fig. 7. It is clear that the intensity of the bands characteristic of NO_3^- (1389, 1764 and 2409 cm^{-1}) was obvious even if the sample was calcined at 673 K. With the increase in the calcination temperature, the band of nitrate on the 15% KNO_3/MCM-48 sample became weaker, indicating the decomposition of KNO_3 at higher temperature [42,45,47]. Obviously the very low intensity of the bands characteristic of NO_3^- obtained at 823 K was attributed to the nearly complete decomposition of KNO_3. Furthermore, there was no OH^- band, observed on either 4% KNO_3/Al_2O_3 or 29% KNO_3/Al_2O_3 after the decomposition of KNO_3 [42], indicating that the decomposition product of KNO_3 was not KOH. Besides, no bands ascribed to NO_2^- (1550 and 1320 cm^{-1}) were detected, demonstrating that the resultant of KNO_3 decomposition was not KNO_2. Taking all the information obtained from the characterizations into account, we can finally conclude that the K_2O species derived from KNO_3 was probably the main active sites. The conclusion coincided with what had been reported; Zhu et al. [42] found that several layers of basic species such as K_2O may overlap on the surface of the alumina when the total amount of KNO_3 dispersed and decomposed on the support has exceeded the monolayer threshold of KNO_3 (ca. 12 wt%). The K_2O derived from KNO_3 was tentatively estimated as the main basic species on KNO_3/Al_2O_3, although K_2O is difficult to detect. Xie et al. [45] had demonstrated that the decomposition products of the loaded KNO_3, forming either K_2O species or Al–O–K group in the composite, were probably the main active sites on KNO_3/Al_2O_3. These results are in good agreement with the CO_2-TPD of KNO_3/MCM-48 demonstrated in Fig. 4. On the other hand, K_2O might sinter and block the pores of mesoporous materials calcined beyond 823 K, most likely owing to this, resulting in a lower basicity together with the loss of the catalytic activity.

3.2.3. *Effect of catalyst dosage*

The effect of catalyst dosage on the DMC conversion and DPC yield is presented in Fig. 8. It was indicated that the improvement

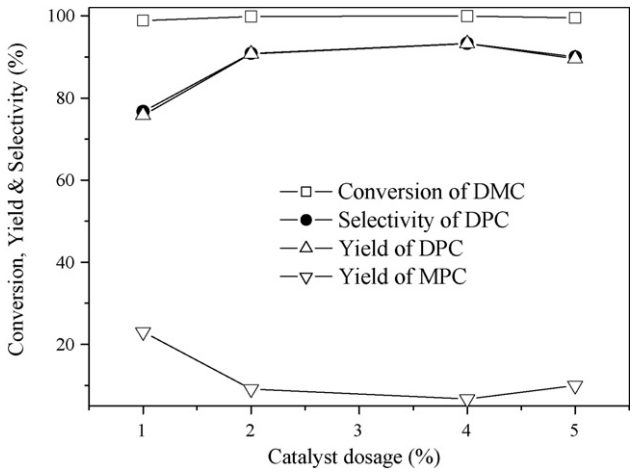

Fig. 8. Effect of the catalyst dosage on conversion of DMC and yield of DPC over 15% KNO_3/MCM-48 at 363 K, reaction time 6 h, feed ratio 4:1 (propanol:DMC) and calcinations temperature 823 K.

of the DMC conversion and DPC yield was not obvious with increasing catalyst dosage. The reasonably high DMC conversion of 98.8% was achieved even though the catalyst dosage was as little as 1%. However, further increase in the catalyst content did not cause a distinct improvement of DMC conversion. The reason was that the main function of the catalyst was to activate propanol. Although the rate of activating propanol was increased with the increase in the catalyst dosage, which caused the increase in the DMC conversion and DPC yield, the visible improvement of catalytic activity was not observed.

3.2.4. Effect of reaction time

The effect of reaction time on the DMC conversion and DPC yield was investigated (Fig. 9). The result indicated that the conversion of DMC and yield of DPC was improved greatly with the increase in reaction time within the first 6 h, and thereafter remained nearly constant near the equilibrium conversion, which was found to be about 99% at 6 h of reaction time.

The results of XRF indicated that potassium was brought into the catalytic system through impregnation. The comparison of the XRF data before and after the catalytic reaction is shown in Table 1. The data exhibited that large amounts of potassium were still maintained in the catalytic system after the reaction, indicating that the active sites of the catalyst were not lost during the reaction time. Therefore, the conversion gradually increased with further lengthening of reaction time from 6 h.

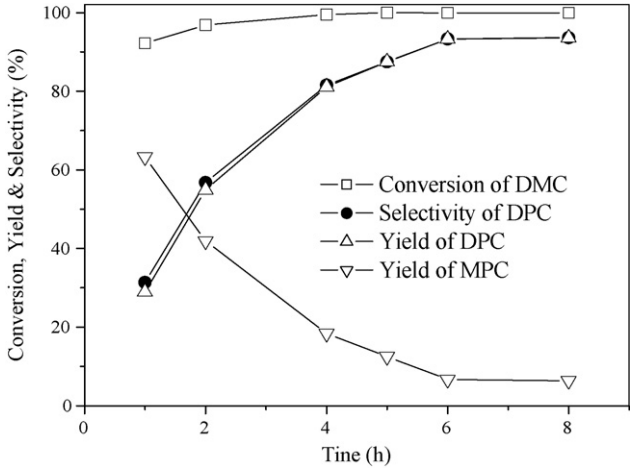

Fig. 9. Effect of reaction time on conversion of DMC and yield of DPC over 15% KNO_3/MCM-48at 363 K, catalyst dosage 5%, feed ratio 4:1 (propanol:DMC) and calcinations temperature 823 K.

Table 1
XRF data for KNO_3/MCM-48 before and after reaction

Catalyst	Element	Mass (%)	Intensity (l/s)
Before reaction	Si	27.69	80.39
	K	64.55	217.84
	Ca	7.76	14.44
After reaction	Si	33.44	89.55
	K	56.10	168.69
	Ca	10.46	19.41

3.3. Comparison of the catalytic activity of KNO_3/MCM-48, KNO_3/Al_2O_3 and KNO_3/NaY

The synthesis of DPC by transesterification of DMC with propanol was carried out over KNO_3/Al_2O_3 and KNO_3/NaY and the results are compared in Table 2. A big difference was observed in the conversion of DMC and selectivity of DPC. The conversion of DMC was up to 98.3% over 15% KNO_3/MCM-48, which was the highest among these catalytic materials, while the selectivities to MPC and DPC were 24.3% and 75.7%, respectively. The selectivity to DPC in the transesterification over 15% KNO_3/MCM-48 was much higher than over either KNO_3/Al_2O_3 or KNO_3/NaY. The KNO_3/Al_2O_3 and KNO_3/NaY catalysts gave similar conversions to DMC, while the selectivity to DPC over KNO_3/Al_2O_3 was higher than over KNO_3/NaY. It is clear that KNO_3/MCM-48 is a much more efficient catalyst for the synthesis DPC than either KNO_3/Al_2O_3 or KNO_3/NaY. From Table 2, we can also find that the properties of the supports were more closely correlated to the catalytic activity. Zhu et al. [42] reported the basicity of alumina and zeolite NaY modified by KNO_3. When the amount of KNO_3 loaded increased to 13 wt%, the basicity of the resulting material was obviously increased and the highest temperature of CO_2 desorption reached 793 K, while the highest temperature peak for CO_2 desorbed from KNO_3/MCM-48 appeared at about 700 K. The CO_2 desorption peak at high temperature was very small in the CO_2-TPD profiles for both KNO_3/Al_2O_3 and KNO_3/MCM-48. It is indicated that there was only little strong basic sites on the three catalysts. It can be seen that the intermediate basic sites on the three catalysts were the main active sites, which were much larger in quantity than the strong basic sites. The sample of KNO_3/MCM-48 shows the main CO_2 desorption peak at 550 K, while the sample of KNO_3/Al_2O_3 only shows the main CO_2 desorption peak at 460 K [42]. When these desorption profiles are compared, it can be seen that the major basic sites of KNO_3/MCM-48 are stronger than those of KNO_3/Al_2O_3 or KNO_3/NaY. It was consistent with the results shown in Table 2.

The BET surface area and pore volume of the catalysts are shown in Table 2. With increasing KNO_3 loading, the surface area and pore volume of KNO_3/Al_2O_3 or KNO_3/NaY decreased sharply. When the loading amount of KNO_3 reached 25 wt%, the surface area of KNO_3/Al_2O_3 and KNO_3/NaY were only 57.6 and 7.3 m^2/g, respectively. It should be noted that the surface area of MCM-48 with a 15 wt% KNO_3 loading was 625.2 m^2/g, which was almost four times as large as the surface area of 12 wt% KNO_3/Al_2O_3 and six times the surface area of 12 wt% KNO_3/NaY. The monolayer threshold of KNO_3 loaded on Al_2O_3 was 12 wt% [42]. Furthermore, the results shown in Table 2 also demonstrate that the pore volume of KNO_3/MCM-48 was much larger than that of KNO_3/Al_2O_3 or KNO_3/NaY. Since the BET surface area and pore volume of KNO_3/MCM-48 are much larger than that of KNO_3/Al_2O_3 or KNO_3/NaY, its much more basic

Table 2
Comparison of catalytic activity[a] of KNO_3/MCM-48, KNO_3/Al_2O_3 and KNO_3/NaY

Catalyst	Potassium loading (%)	BET surface areas (m^2/g)	Pore volume (cm^3/g)	DMC conversion (%)	MPC selectivity (%)	DPC selectivity (%)
KNO_3/Al_2O_3	5	164.4	0.39	62.9	70.3	29.7
	12	134.6	0.28	58.2	60.3	39.7
	25	57.6	0.005	58.5	68.4	31.6
KNO_3/NaY	5	348.4	0.22	63.9	90.4	9.6
	12	98.3	0.09	67.3	93.5	6.5
	25	7.3	0.018	60.3	76.2	23.8
KNO_3/MCM-48	15	625.2	0.78	98.3	24.3	75.7

[a] Reaction conditions: catalyst dosage 1%, reaction time 6 h, feed ratio 4:1 (propanol:DMC), calcination temperature 873 K, reaction temperature 363 K.

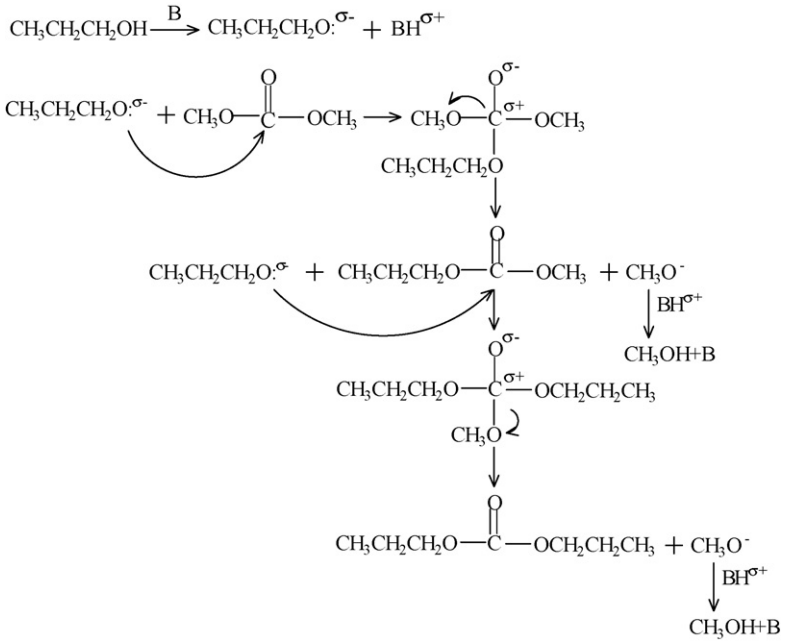

Scheme 1. A plausible reaction mechanism.

sites can be attributed to it large BET surface area and pore volume.

The large surface area and large pore volume are in favor of the dispersion of the active sites and the diffusion of reactants, which may cause a high catalytic activity in liquid-phase reactions. Because of the large surface area and large pore volume, along with the more active sites generated by KNO_3 on MCM-48, KNO_3/MCM-48 exhibited the highest DMC conversion and DPC selectivity among these catalysts. Because of its larger surface area and pore volume KNO_3/Al_2O_3 demonstrated a higher selectivity to DPC than KNO_3/NaY, though they exhibited similar basicity. Apparently, the selectivity to DPC was not only influenced by the basicity of the catalyst, but also related to the BET surface area and pore volume of the catalyst.

3.4. Suggested mechanism

As shown in Scheme 1, the mechanism of the transesterification of dimethyl carbonate with propanol to synthesize DPC over KNO_3/MCM-48 was proposed. Propanol was adsorbed on the basic sites of KNO_3/MCM-48 (represented as B) to form a nucleophilic anion ($CH_3CH_2CH_2O^-$). Then the carbonyl carbon of DMC was attacked by the nucleophilic anion ($CH_3CH_2CH_2O^-$) and an activated complex containing the carbocation was produced. Ester exchange was completed along with the formation of methanol and methyl propyl carbonate (MPC). A further nucleophilic reaction between nucleophilic anion ($CH_3CH_2CH_2O^-$) and methyl propyl carbonate yields the DPC.

4. Conclusions

The MCM-48 supported KNO_3 catalytic system exhibited very high catalytic activity in the synthesis of DPC by transesterification of DMC with propanol. The effect of potassium loadings, calcination temperature, catalyst dosage and reaction time exhibited regular trends on the DMC conversion and DPC yield. It was indicated that the catalyst KNO_3/MCM-48 showed very high catalytic activity under the optimized reaction conditions. The highest DMC conversion, DPC selectivity and DPC yield were 99.9%, 93.4% and 93.3%, respectively.

Acknowledgement

We deeply appreciate the financial support from the National Basic Research Priorities Programme of China (2003CCA03200).

References

[1] A.G. Shaikh, Chem. Rev. 96 (1996) 951.
[2] M.A. Pacheo, C.L. Marshall, Energy Fuels 11 (1991) 2.
[3] D. Delledonne, F. Rivetti, U. Romano, Appl. Catal. A: Gen. 221 (2001) 241.
[4] Y. Ono, Catal. Today 35 (1997) 15.
[5] Y. Ono, Appl. Catal. A: Gen. 155 (1997) 133.

[6] S.A. Anderson, W.R. Thatcher, J. Mol. Catal. A: Chem. 220 (2004) 247.
[7] Z. Li, K.C. Xie, C.T. Robert, Appl. Catal. A: Gen. 205 (2001) 85.
[8] T. Wei, M.H. Wang, W. Wei, Y.H. Sun, B. Zhong, Fuel Process. Technol. 83 (2003) 175.
[9] C.F. Li, S.H. Zhong, Catal. Today 82 (2003) 83.
[10] C.S. Chin, D. Shin, G. Won, J. Ryu, H.S. Kim, B.G. Lee, J. Mol. Catal. A: Chem. 160 (2000) 315.
[11] P. Yang, Y. Cao, J.C. Hu, W.L. Dai, K.N. Fan, Appl. Catal. A: Gen. 241 (2003) 363.
[12] X.B. Ma, H.L. Guo, S.P. Wang, Y.L. Sun, Fuel Process. Technol. 83 (2003) 275.
[13] M.S. Han, B.G. Lee, B.S. Ahn, D.J. Moon, S.I. Hong, Appl. Surf. Sci. 211 (2003) 76.
[14] M.S. Han, B.G. Lee, B.S. Ahn, H.S. Kim, D.J. Moon, S.I. Hong, J. Mol. Catal. A: Chem. 203 (2003) 137.
[15] Z.H. Fu, Y. Ono, J. Mol. Catal. A: Chem. 118 (1997) 293.
[16] A. Rodríguez, J. Canosa, J. Tojo, J. Chem. Thermodyn. 33 (2001) 1383.
[17] V. Pokhakar, S. Sivaram, Polymer 36 (1995) 4851.
[18] S.P. Wang, X.B. Ma, H.L. Guo, J.L. Gong, X. Yang, G.H. Xu, J. Mol. Catal. A: Chem. 214 (2004) 273.
[19] W.Q. Zhou, X.Q. Zhao, Y.J. Wang, J.Y. Zhang, Appl. Catal. A: Gen. 260 (2004) 19.
[20] Q. Cai, H.B. Zhang, W.Y. Lin, W.Q. Pang, Chem. J. Chin. Univ. 20 (1999) 675.
[21] S.R. Zhai, M. Pu, Y. Zhang, D. Wu, Y.H. Sun, Acta Phys.-Chem. Sin. 19 (2003) 167.
[22] S.G. Wang, D. Wu, Y.H. Sun, B. Zhong, Mater. Res. Bull. 36 (2001) 1717.
[23] J.C. Varitu, A. Malek, W.J. Roth, C.T. Kresge, S.B. McCullen, Microporous Mesoporous Mater. 44–45 (2001) 691.
[24] N. Nishiyama, H. Saputra, D.H. Park, Y. Egashira, K. Ueyama, J. Membr. Sci. 218 (2003) 165.
[25] J. Parmentier, J. Patarin, J. Dentzer, C.V. Guterl, Ceram. Int. 8 (2002) 1.
[26] D. Kumar, S. Bera, A.K. Tripathi, G.K. Dey, N.M. Gupta, Microporous Mesoporous Mater. 66 (2003) 157.
[27] R. Köhn, D. Paneva, M. Dimitrov, T. Tsoncheva, I. Mitov, C. Minchev, M. Fröba, Microporous Mesoporous Mater. 63 (2003) 125.
[28] Q.R. Peng, Y. Yang, Y.Z. Yuan, J. Mol. Catal. A: Chem. 219 (2004) 175.
[29] H. Gies, S. Grabowski, M. Bandyopadhyay, W. Grünert, O.P. Tkachenko, K.V. Klementiev, A. Birkner, Microporous Mesoporous Mater. 60 (2003) 31.
[30] P. Selvam, S.E. Dapurkar, Appl. Catal. A: Gen. 276 (2004) 257.
[31] S.E. Dapurkar, P. Selvam, J. Catal. 224 (2004) 178.
[32] J.L. Shen, Y.C. Lee, Y.L. Liu, C.C. Yu, P.W. Cheng, C.F. Cheng, Microporous Mesoporous Mater. 64 (2003) 135.
[33] K. Hadjiivanov, T. Tsoncheva, M. Dimitrov, C. Minchev, H. Knözinger, Appl. Catal. A: Gen. 241 (2003) 331.
[34] Y.C. Lee, Y.L. Liu, J.L. Shen, I.J. Hsu, P.W. Cheng, C.F. Cheng, C.H. Ko, J. Non-Cryst. Solids 341 (2004) 16.
[35] C.H. Subrahmanyam, B. Viswanathan, T.K. Varadarajan, J. Mol. Catal. A: Chem. 226 (2005) 155.
[36] C.B. Murray, C.R. Kagan, M.G. Bawendi, Science 270 (1995) 1335.
[37] G. Oye, J. Sjoblom, M. Stocker, Microporous Mesoporous Mater. 27 (1999) 171.
[38] S. Brunauer, P.H. Emmett, E. Teller, J. Am. Chem. Soc. 60 (1938) 309.
[39] C.Y. Chen, H.X. Li, M.E. Davis, Microporous Mater. 2 (1993) 17.
[40] C.T. Kresge, M.E. Leonowicz, W.J. Rotj, Nature 359 (1992) 710.
[41] J. Fung, I. Wang, Appl. Catal. A: Gen. 166 (1998) 327.
[42] J.H. Zhu, Y. Wang, Y. Chun, X.S. Wang, J. Chem. Soc., Faraday Trans. 94 (1998) 1163.
[43] X.B. Ma, S.P. Wang, J.L. Gong, X. Yang, G.H. Xu, J. Mol, Catal. A: Chem. 222 (2004) 183.
[44] L.B. Sun, Y. Chun, F.N. Gu, M.B. Yue, Q. Yu, Y. Wang, J.H. Zhu, Mater. Lett. 61 (2007) 2130.
[45] W.L. Xie, H. Peng, L.G. Chen, Appl. Catal. A: Gen. 300 (2006) 67.
[46] D.E. Jiang, G.C. Pan, B.Y. Zhao, G.P. Ran, Y.C. Xie, E.Z. Min, Appl. Catal. A: Gen. 201 (2000) 169.
[47] C. Yuan, J.H. Zhu, Y. Wang, Q.H. Xu, Chin. Sci. Bull. 43 (1998) 721.